Effects of debris-flow magnitude-frequency distribution on avulsions and fan development

T. de Haas[1,2], A. Kruijt[2], A. L. Densmore[1]

[1]Department of Geography, Durham University, Durham, UK.
[2]Faculty of Geosciences, Universiteit Utrecht, Utrecht, The Netherlands.

Corresponding author: T. de Haas, tjalling.de-haas@durham.ac.uk

Abstract

Shifts in the active channel on a debris-flow fan, termed avulsions, pose a large threat because new channels can bypass mitigation measures and cause damage to settlements and infrastructure. Recent, but limited, field evidence suggests that avulsion processes and tendency may depend on the flow-size distribution, which is difficult to constrain in the field. Here, we investigate how the flow magnitude-frequency distribution and the associated flow-magnitude sequences affect avulsion on debris-flow fans. We created three experimental fans with contrasting flow-size distributions: (1) a uniform distribution, (2) a steep double-Pareto distribution with many flows around the mean and a limited number of large flows, and (3) a shallow double-Pareto distribution with fewer flows around the mean and more abundant large flows. The fan formed by uniform flows developed through regular sequences of stepwise channelization, backstepping of deposition toward the fan apex, and avulsion over multiple flows. In contrast, the wide range of sizes in the double-Pareto distributions led to distinct avulsion mechanisms and fan evolution. Here, large flows could overtop channels, creating levee breaches that could initiate avulsion immediately or in subsequent events. Moreover, sequences of small- to moderately-sized flows could deposit channel plugs, triggering avulsion in the next large flow. This mechanism was most common on the fan formed by a steep double-Pareto distribution but was rare on the fan formed by a shallow double-Pareto distribution, where large flows were more frequent. We infer that some flow-size distributions are more likely to cause avulsions - especially those that produce abundant sequences of small flows followed by a large flow. Critically, avulsions in our experiments could occur by either large single events or over multiple flows. This observation has important implications for hazard assessment on debris-flow fans, suggesting that attention should be paid to flow history as well as flow size.

1 Introduction

Debris-flow fans are ubiquitous landforms in high-relief areas around the world [e.g., *Beaty*, 1963; *Okuda et al.*, 1981; *Whipple and Dunne*, 1992; *Blair and McPherson*, 1994, 2009; *De Haas et al.*, 2014, 2015a; *D'Arcy et al.*, 2015; *Schürch et al.*, 2016]. They form by deposition in repeated debris flows, and are thus an archive of past flow magnitude, timing, composition and depositional pattern [*Schumm et al.*, 1987; *Harvey*, 2011; *Dühnforth et al.*, 2007]. Extracting such information requires understanding of the spatio-temporal patterns of debris-flow fan evolution, which largely depend on changes in the active-channel position, termed avulsions, that distribute sediment across the fan surface [*Schürch et al.*, 2016].

Ongoing expansion of human populations into mountainous regions has led to increasing exposure to debris-flow hazards [*Pederson et al.*, 2015]. Avulsions pose an especially severe threat to settlements and other infrastructure on fans, particularly as flow mitigation measures such as check dams and retention basins are typically applied to active channels and cannot prevent damage from flows that establish a new channel pathway. The mechanisms by which debris flows avulse to occupy new flow paths on fans, however, and the controls on avulsion frequency and timing, are poorly understood [e.g., *Pederson et al.*, 2015; *De Haas et al.*, 2016, 2018]. One outstanding issue is that the spatio-temporal patterns of deposition on debris-flow fans have been monitored [*Suwa and Okuda*, 1983; *Wasklewicz and Scheinert*, 2016; *Imaizumi et al.*, 2016] or reconstructed [e.g., *Helsen et al.*, 2002; *Dühnforth et al.*, 2008; *Stoffel et al.*, 2008; *Bollschweiler et al.*, 2008; *Schürch et al.*, 2016; *Zaginaev et al.*, 2016] on only a few natural debris-flow fans. Moreover, there have been few attempts to simulate debris-flow fan evolution with physical scale experiments [*Hooke*, 1967; *Schumm et al.*, 1987; *De Haas et al.*, 2016] or numerical models [*Schürch*, 2011]. *De Haas et al.* [2018] summarized and compared the patterns of spatio-temporal debris-flow deposition on natural fans, and identified two important controls on avulsion that operate over separate time scales: (1) during individual flows or flow surges, deposition of sediment locally blocks or plugs channels, forcing avulsion in subsequent flows, and (2) over time scales of tens of flows, the average locus of debris-flow deposition gradually shifts towards topographically lower sectors of a fan. Many, but not all, debris-flow avulsions follow a pattern of channel plugging, backstepping of deposition toward the fan apex, avulsion and establishment of a new active channel. In this conceptual model, sequences of small- to medium-sized flows can progressively deposit sediment within the active channel toward the fan apex, thereby plugging the channel, until a flow occurs that is of sufficient magnitude to leave the main channel upstream of the sediment plug and form a new channel.

Plug deposition is a stochastic process that depends on the sequence of flow magnitudes, the geometry of the channel, and the composition and bulk rheology of the flows. Furthermore, *De Haas et al.* [2018] showed that large flows can have contrasting impacts on avulsion, depending on whether or not they follow smaller flows that have deposited channel plugs.

These observations suggest that avulsions and associated patterns of debris-flow fan formation may depend on the relative numbers of small and large flows - and thus on the magnitude-frequency distribution - and on the sequence of flows that feed a fan. Each debris-flow fan is built by a unique, but generally unknown, magnitude-frequency distribution, which could conceivably lead to contrasting spatio-temporal avulsion patterns on different fans. While *De Haas et al.* [2018] speculated on this link, they lacked robust data on flow volumes for most of their field examples, and they had no information on the underpinning distributions. For hazard mitigation, and to effectively decipher the debris-flow fan archive, it is therefore of key importance to understand how different magnitude-frequency distributions, and the associated sequences of flow sizes, can affect avulsions and the spatio-temporal patterns of debris-flow fan evolution. This is especially relevant in regions where magnitude-frequency distributions have changed, or may change, as a result of global climate change [e.g., *Rebetez et al.*, 1997; *Stoffel*, 2010; *Clague et al.*, 2012] or regional factors such as earthquakes [e.g., *Shieh et al.*, 2009; *Huang and Fan*, 2013; *Ma et al.*, 2017], landslides [e.g., *Imaizumi et al.*, 2016], or wildfires [e.g., *Cannon et al.*, 2008, 2011].

Here, we investigate how flow magnitude-frequency distribution and associated flow sequences affect the spatio-temporal patterns of debris-flow-fan development. To do so, we study and compare the evolution, avulsion mechanisms and compensational tendency of three experimentally-created debris-flow fans formed by different flow-magnitude distributions. We follow *De Haas et al.* [2016], who investigated avulsions and debris-flow fan evolution on an experimental fan formed by flows of uniform size and composition. They found that avulsions on this fan followed a predictable pattern of gradual backstepping, avulsion and channelization. Phases of backstepping and channelization were approximately equal in length and developed over multiple flows. They speculated about the potential effects of varying flow size on avulsion occurrence and mechanism, but could not test these ideas. We thus build on this work by creating two additional debris-flow fans formed by contrasting heavy-tailed magnitude-frequency distributions using the same experimental setup, and comparing the avulsion mechanisms and spatio-temporal patterns of activity between these fans.

The structure of this paper is as follows. We first describe the methodology, experimental setup and procedure, and data reduction and analysis methods. Then we describe the spatio-temporal patterns of development on the three experimental debris-flow fans, and determine their compensational tendencies as quantified by the compensation index [cf. *Straub and Pyles*, 2012]. Finally, we discuss the potential relationships between debris-flow magnitude-frequency distribution, flow sequence, and avulsion on debris-flow fans, based on the experimental results.

2 Materials and methods

The fan described by *De Haas et al.* [2016] and the two new experimental fans described here were generated with the same experimental setup and procedure. The large-scale flow patterns of the experimental debris flows mimic those of natural debris flows [*De Haas et al.*, 2015b]: all experimental debris flows presented here were frictional flows, with coarse particles selectively transported to the flow front and subsequently shouldered aside to form coarse-grained lateral levees. Each flow produced a distinct depositional lobe wherein coarse particles were predominantly concentrated at the frontal flow margins [*De Haas et al.*, 2015b; *De Haas and Van Woerkom*, 2016]. Moreover, channel width to depth ratios, and runout length and area relative to debris-flow volume, are similar to those in natural debris flows [*De Haas et al.*, 2015b]. The morphological similarity between the experimental and natural debris flows allows for representative interactions between debris flows and evolving fan morphology, which enables us to study avulsion mechanisms and tendencies, and allows for broad comparisons of the results to natural debris-flow fans [cf. *Hooke and Rohrer*, 1979; *Paola et al.*, 2009]. We emphasize that the experiments are not intended as scaled analogues of natural flows or fans, and that our aim is to examine the morphodynamic behavior of the system in the face of different flow-magnitude distributions. Thus, it are the differences between experiments, rather than the detailed results of a single experiment, that are of primary interest.

2.1 Experimental setup and procedure

The experimental setup was described in detail in *De Haas et al.* [2016], and consisted of a mixing tank connected to a 30° inclined chute channel, 2 m long and 0.12 m wide, which at its downstream end was linked to an outflow plain with an inclination of 10° (Fig. 1). The channel bed and sidewalls of the chute channel were covered with sandpaper to simulate natural bed roughness (grade 80; average particle diameter 0.19 mm), and the outflow plain was covered by a 0.5 cm deep layer of unconsolidated sand (median particle diameter 0.4 mm). Sediment and water were added to the mixing tank and then agitated until a coherent mixture was formed, after which a gate was opened electromagnetically to release the debris-flow mixture into the channel. A hatch in the channel bed, located 0.76 m above the transition from the channel to the outflow plain, was opened electromagnetically 1.5 s after the release of debris from the mixing tank to cut off the sediment-poor debris-flow tail, which would otherwise incise unrealistically deep into the fan deposits [*De Haas et al.*, 2016].

The experimental fans were created by stacking of consecutive debris-flow deposits on the outflow plain, leaving base level fixed. The fans were allowed to grow in size until a maximum extent was reached, at which point subsequent debris flows were not able to reach the fan as they were blocked by accumulated debris in the feeder channel. This occurred after 55 to 85 flows, depending on the experiment. All debris flows had a similar composition consisting of clay (kaolinite; 5.8% of total sediment volume), sand (77.2% of the total sediment volume) and basaltic gravel (17% of the total sediment volume) (Fig. 2). All flows contained 44 vol% of water.

Above the flume, a digital camera (Canon PowerShot A640) was set up to image fan topography after each flow. Videos of flow movement and deposition on the fan were captured with a Canon Powershot A650 IS on a tripod directed obliquely at the channel and fan. Deposit morphology was measured at sub-millimeter resolution and accuracy after every debris-flow event using a Vialux z-Snapper 3D scanner that captures a three-dimensional point cloud from a fringe pattern projector [*Hoefling*, 2004]. Point clouds from the scanner were converted into a gridded digital elevation model (DEM) with 1 mm spatial resolution using natural neighbor interpolation (Fig. 1).

2.2 Magnitude-frequency distribution

The three experimental fans were formed by selecting flow sizes from three different magnitude-frequency distributions (Fig. 3). Although the distribution of flow magnitudes from natural debris-flow catchments is generally not known [e.g., *Stoffel*, 2010], there is a considerable body of evidence that landslide magnitudes follow a heavy-tailed distribution [e.g., *Hovius et al.*, 1997; *Hungr et al.*, 1999; *Dai and Lee*, 2001; *Stark and Hovius*, 2001; *Malamud et al.*, 2004; *Bennett et al.*, 2012]. Given the genetic link between shallow landsliding and debris-flow initiation [e.g., *Iverson*, 1997; *Iverson et al.*, 2011; *Bennett et al.*, 2013], it seems logical to assume that debris-flow magnitudes may also show heavy-tailed behavior. Indeed, *Bardou and Jaboyedoff* [2008] demonstrated a heavy-tailed magnitude distribution for a compilation of historical debris flows from the Swiss Alps, while *Bennett et al.* [2014] compiled observations from the Illgraben (Switzerland) that also show heavy-tailed behavior. *Bennett et al.* [2014] also cautioned, however, that their modeling showed important differences between the magnitude distributions of landslides and debris flows in the Illgraben catchment.

With these considerations in mind, we developed and compared three distinct flow-magnitude distributions: a uniform distribution previously described by *De Haas et al.* [2016] (fan 01), a heavy-tailed distribution with a large power-law exponent (corresponding to a rapid decrease in exceedance probability with increasing flow magnitude, fan 02), and a heavy-tailed distribution with a small exponent (corresponding to a more gradual decrease in exceedance probability with increasing magnitude, fan 03). For convenience, we extracted flow mass from each distribution, using a constant flow composition and thus bulk density. To simulate the two heavy-tailed distributions, we followed *Stark and Hovius* [2001] and *Guthrie and Evans* [2004] in adopting a double-Pareto formulation. This distribution exhibits power-law behavior in the upper and lower tails, and allows for inclusion of a rollover, with extremely large and extremely small flows both being less likely [e.g., *Reed*, 2001; *Reed and Jorgensen*, 2004]. The probability density function can be written as:

$$f(M) = \begin{cases} \frac{\alpha\beta}{\alpha+\beta}\left(\frac{M}{M_c}\right)^{\beta-1}, M \leq M_c \\ \frac{\alpha\beta}{\alpha+\beta}\left(\frac{M}{M_c}\right)^{-\alpha-1}, M \geq M_c \end{cases} \tag{1}$$

where M is flow mass (kg), M_c is a rollover parameter (kg), and α and β are empirical constants that describe the slope of the density function at small and large magnitudes, respectively. For fan 02, we set M_c = 4.25 kg, α = 10.05, and β = 30.5, and we refer to this below for convenience as the 'steep' distribution. For fan 03, we set M_c = 3.0 kg, α = 3.05, and β = 10.5, and we refer to this as the 'shallow' distribution. These distributions are not intended to mimic known field examples, but were rather designed as plausible and contrasting end-members.

The mean flow mass in all three experiments was fixed at 6.5 kg. For fan 01, the flow mass was kept uniform. For fans 02 and 03, the mass of each flow in the sequence was determined by extracting a random deviate from the distribution described by eq. 1 with the appropriate parameter values. The maximum flow mass in the latter experiments was fixed at 13 kg due to operational constraints.

2.3 Data reduction

2.3.1 Spatio-temporal patterns of activity

The patterns of deposition in each flow were summarized by the flow angle and runout distance for each debris-flow snout, the maximum runout among all snouts, the deposit width, the deposit width/depth ratio, and the channel depth at the fan apex (Fig. 4). The flow angle was defined as the angle between the fan midline and a straight line connecting the fan apex and the debris-flow snout. The runout distance per snout was defined as the length of a straight line from apex to snout. Deposit width was defined as the maximum width of the deposit, excluding individual snouts substantially outside of the main flow direction. Apex channel depth was measured 10 cm downstream of the fan apex.

2.3.2 Compensation index

The compensation index (κ_{cv}) describes the tendency of a sedimentary system to occupy and fill topographic lows by avulsion [*Straub et al.*, 2009; *Wang et al.*, 2011; *Straub and Pyles*, 2012]. This index ranges from 0 to 1, representing a continuum from persistent channel positions and vertical (anti-compensational) stacking of deposits (κ_{CV} = 0), through random channel positions (κ_{CV}= 0.5), to frequent avulsions and perfect topographic compensation (κ_{CV} = 1). In other words, in an anti-compensational system previous deposits act as attractors for the active channel, while in a compensational system previous deposits act as deflectors. As such, the compensation index is a valuable measure for understanding avulsion frequency and future flow path prediction. For the experimental debris-flow fans we calculated the compensation index at 0.05 m increments of distance from fan apex to fan toe following the method of *Straub and Pyles* [2012], which is a revised version of the earlier approach of *Straub et al.* [2009] that ignores basin subsidence rates. This index has been previously used to calculate the compensational tendency of natural debris-flow fans in Colorado, USA, by *Pederson et al.* [2015]. The compensation index depends upon the coefficient of variation of the ratio of local to mean sediment thickness between every pairwise combination of bed boundaries integrated across the horizontal length (L) of the basin:

$$CV = \left(\int_L \left[\frac{\Delta\eta(x)_{A,B}}{\Delta\bar{\eta}_{A,B}} - 1 \right]^2 dL \right)^{0.5} \tag{2}$$

where $\Delta\eta(x)_{A,B}$ is the local sediment thickness between surfaces A and B, and $\Delta\bar{\eta}_{A,B}$ is the mean deposit thickness between surfaces A and B. The compensation index (κ_{cv}) is the exponent in the power law decay of CV with increasing mean sediment thickness:

$$CV = a\Delta\bar{\eta}_{A,B}{}^{-\kappa_{cv}} \tag{3}$$

where a is an empirical constant.

3 Results

3.1 Spatio-temporal patterns of fan development

In this section we summarize the spatio-temporal evolution of the three experimental debris-flow fans and their dominant avulsion mechanisms - more extensive descriptions of the evolution of the fans on a flow by flow basis can be found in the supplementary materials. We end the results by presenting the compensation index calculations. Flow sizes and spatio-temporal patterns of debris-flow activity on the fans are summarized in Figure 5. Flows that moved towards the left-hand side of the fan, when looking downstream from the fan apex, are denoted by negative flow angles and flows towards the right are denoted by positive flow angles.

3.1.1 Fan 01: Uniform distribution

Fan 01 evolved in a predictable manner (Figs. 5a-f, 6; supplementary movie S1): filling of accommodation induced backstepping sequences which resulted in a searching phase, followed by avulsion and re-channelization (Fig. 6). Maximum runout was observed to decrease in gradual and near-uniform steps over multiple flows during the backstepping phases, and similarly increased during phases of channel establishment and progradation (Fig. 5b). These progradation and backstepping phases required an approximately similar number of flows, but the total length of these phases increased as the fan apex grew in elevation and more accommodation had to be filled before a backstepping sequence could be initiated (compare the sequence during flows 10-25 with 25-52 in Figs. 5a and supplementary movie S1). During searching phases, when multiple channels were active, deposit width was relatively large while the apex channel was shallow or even absent (Fig. 5c-e) [see *De Haas et al.*, 2016, for further details].

3.1.2 Fan 02: Steep double-Pareto distribution

Runout distances on fan 02 were relatively long during channelized phases and restricted during unchannelized phases (Figs. 5g-l, 7; supplementary movie S2). Compared to fan 01, however, this relationship was less well-developed as a result of the varying debris-flow sizes. Periods of backstepping and the formation of persistent channel plugs that induced avulsion on fan 02 were generally initiated by (1) sequences of small- to moderately-sized flows (e.g., flows 16-18, 26-29 and 35-36; Fig. 7a-h; supplementary movie S2), and by (2) complete filling of the regional accommodation (e.g., flows 53-58). Very large events (e.g., flows 15 and 59; Fig. 7j) had sufficient magnitude to overflow the main channel, often upstream of channel plugs, and form a new channel. Additionally, large flows were often observed to overtop the main channel in multiple locations, creating levee breaches that could be exploited as avulsion sites during subsequent flows and develop into new main channels.

3.1.3 Fan 03: Shallow double-Pareto distribution

Runout on fan 03 was generally greatest when a well-defined apex channel was present (Figs. 5m-r, 8; supplementary movie S3). During searching phases when channel depth was small or an apex channel was absent, runout was restricted and deposits were wide. This trend is only weak and hard to recognize, however, due to the large variation in runout and deposit width caused by the broad distribution of flow magnitudes. Channels were more persistent on fan 03 compared to fans 01 and 02, and small channel plugs were sometimes removed by large flows (Fig. 8a-d). Clear backstepping sequences over multiple flows in the main channel, which were frequently observed on fans 01 and 02, were much less frequent on fan 03. Backstepping and plug deposition were, however, generally responsible for the closure of secondary channels. Periods during which the main locus of deposition migrated towards the fan apex did occur and were observed to induce avulsion (e.g., flows 56-62; Fig. 8e-f), but these backstepping sequences predominantly occurred as a result of filled regional accommodation. Moreover, these sequences were irregular, often showing alternating progradation and retrogradation on an event scale, because of the strongly varying flow sizes. New topographically-favorable channels were often formed during solitary large events (e.g., flows 63-64 and 69; Fig. 8h), triggering main channel avulsion in subsequent flows.

3.2 Compensational tendency

In this section we calculate the compensation index (eq. 3) for the experimental debris-flow fans. We first describe the stratigraphy that developed in each experiment at representative proximal and distal transects located 0.2 and 0.8 m downstream of the apex, respectively. Next, we determine the compensation index and examine how it varied with distance from the apex in each experiment.

3.2.1 Fan stratigraphy

On fan 01, stratigraphy on both the proximal and distal parts of the fan shows that deposition was generally persistent for periods of at least $\sim$20 flows, after which activity avulsed to a topographically lower area (Fig. 9a-b). Fan 02 showed roughly similar behavior, but the variability in debris-flow magnitudes resulted in less clearly-pronounced lateral shifts and a larger number of overflow events in the fan stratigraphy (Fig. 9c-f). We define an overflow event as a flow that was able to extensively overtop the main channel levees and deposit substantial amounts of sediment adjacent to the main channel. Overflow events were even more pronounced in the stratigraphy of fan 03 compared to fans 01 and 02, as would be expected from the shallow flow distribution. This difference resulted in even more persistent deposition and less pronounced lateral shifts in both the proximal and distal parts of the fan. Deposition was observed to be persistent on one side of the fan for $\sim$20 flows on fans 01 and 02, while it was typically persistent for $>$30 flows on fan 03 (Figs 5, 9).

3.2.2 Compensation index

The compensation index was roughly similar on the three experimental debris-flow fans (Fig. 10). In general, the index had a value of $\sim$0.25 near the fan apex, and increased roughly linearly to $\sim$0.35 near the fan toe. The compensation index was well-defined and similar for stratigraphic intervals of between 1 and 20 flows, implying that the compensational behavior was similar over this range of depositional scales.

4 Discussion

In this section we discuss the effects of the flow magnitude-frequency distribution and associated flow-magnitude sequence on avulsion and experimental fan evolution, and compare these findings to observations from natural debris-flow fans. Next, we consider the compensational tendencies of debris-flow fans, and implications for flow routing. Finally, we detail the potential implications of our experimental results for mitigation of avulsion hazards on debris-flow fans.

4.1 Effects of magnitude-frequency distribution on avulsion mechanisms and fan evolution

Broadly speaking, the three experimental fans followed similar overall patterns of development. After a spin-up phase during which flow deposits were largely stacked on top of each other along the fan midline, each fan showed an alternation of (1) channelized phases, during which debris flows occupied a well-defined channel and deposited on the medial to distal parts of the fan, and (2) unchannelized or searching phases, during which flows were spread widely over the proximal parts of the fan and formed multiple snouts. The searching phases continued until debris-flow activity avulsed towards a topographically-favorable sector of the fan. All experimental fans occupied an increasing number of channels and formed more snouts as the fan surface topography grew more complex over time. Most of these channels were closed off and abandoned by sequences of backstepping sedimentation over the course of multiple debris flows.

The three different flow distributions also caused marked differences, however, in avulsion mechanisms and patterns of fan evolution. Fan 01, with uniform flow magnitudes, developed through regular sequences of stepwise channelization, backstepping, and avulsion over multiple flows *De Haas et al.* [2016]. On this fan, backstepping of deposition proceeded from fan toe to fan apex before substantial shifts in main channel location could occur. This sequence and the filling of regional accommodation is analogous to the backfilling process that causes avulsion on fluvial-flow-dominated fans [e.g., *Van Dijk et al.*, 2009, 2012; *Clarke et al.*, 2010; *Powell et al.*, 2012; *Hamilton et al.*, 2013]. In contrast, large debris flows on fans 02 and 03 were able to overtop channel levees and either occupy new flow paths, or trigger avulsion in subsequent flows. As a result, avulsions could occur during a single flow of sufficient magnitude, whereas avulsions on fan 01 always occurred over multiple flows. In addition, large events could cause widespread overbank surges, thereby also contributing to fan construction and channel embankment. This was particularly evident on fan 03, which had a shallow power-law decay and thus had relatively more abundant large flows than the other two experiments.

Avulsions on fans 02 and 03 were also triggered by specific sequences of flow sizes that promoted channel plugging and backstepping, enabling rapid channel closure and avulsion without the need for complete backstepping sequences from fan toe to apex. These sequences generally consisted of a series of flows with similar or progressively-decreasing sizes (e.g., backstepping sequences during flows 15-19 and 25-29, and channel plug sequence during flows 35-36, on fan 02). Interestingly, these sequences were more common on fan 02 compared to fan 03, which we attribute to both (1) the predominance of small to moderate flows on fan 02 and (2) the relative abundance of large flows on fan 03, which kept the channel swept clean.

These experimental observations suggest that new channels on debris-flow fans can form instantaneously during large flows, but can also form progressively during sequences of small- to medium-sized flows. New channels generally form after channel blocking by a backstepping sequence, which is either initiated by (1) the deposition of a channel plug or (2) filling of regional accommodation. In the latter mechanism, sedimentation occurs over the near-full length of the channel, whereas large parts of the abandoned channel, downstream of the plug, are preserved by the former mechanism; this distinction may be important for routing of future flows down the abandoned channel network [e.g., *Aslan et al.*, 2005; *Reitz et al.*, 2010; *De Haas et al.*, 2018]. The relative importance of these two mechanisms for channel abandonment appears to depend largely on the debris-flow magnitude-frequency distribution: on fan 02 most backstepping sequences were initiated by channel plugs formed during favorable sequences of small- to medium-sized flows, while the absence of variable flow magnitudes on fan 01 and the relative abundance of large flows on fan 03 both (partly) inhibited the formation of channel plugs.

The observed spatio-temporal patterns of development on the experimental debris-flow fans are similar to patterns observed on natural debris-flow fans. Channel plugs locally block channels and force subsequent flows to avulse on the experimental fans (Fig. 7a-c), and this behavior is also frequently observed in natural fan systems [*Okuda et al.*, 1981; *Suwa and Yamakoshi*, 1999; *De Haas et al.*, 2018] (Fig. 11b). Over time scales of multiple events, typically at least 5 to >20 flows on both a range of natural debris-flow fans [*Okuda et al.*, 1981; *Suwa et al.*, 2009; *Imaizumi et al.*, 2016; *De Haas et al.*, 2018] and in the experiments, the average locus of debris-flow deposition shifts towards the topographically lower parts of a fan (Fig. 12). Moreover, in both our experiments and on natural debris-flow fans [*De Haas et al.*, 2018], avulsion and new channel formation predominantly occur as a result of large flows, especially when these follow channel-plug formation in previous flows or when they occupy multiple channels that can then become established as a new favorable pathway [*Stoffel et al.*, 2008; *Imaizumi et al.*, 2016]. By way of comparison, avulsions on fluvial fans are often triggered during high flood discharges [e.g., *Brizga and Finlayson*, 1990; *Slingerland and Smith*, 1998; *Edmonds et al.*, 2009; *Reitz et al.*, 2010; *Ganti et al.*, 2016], and the avulsion frequency on deltas has been shown to increase with increasing discharge variability in the delta branches [*Ganti et al.*, 2014]. These common observations emphasize the link between the magnitude-frequency distribution of formative flows and avulsion frequency across a wide range of distributary systems.

It is important to temper our interpretations with several caveats. Our experiments show that avulsion behavior is highly sensitive to the sequence of flow sizes in a series of successive events. A single magnitude-frequency distribution can, of course, yield contrasting sequences of flow sizes. We thus anticipate that repeating our experiments, randomly extracting flow magnitudes from a fixed distribution, may result in contrasting fan development. What is important here, however, is the way in which avulsions develop over short sequences of flows; we are interested in the underlying mechanisms by which avulsions occur, not in the final morphology of the experimental fans. Similar sequences should give rise to similar mechanisms, irrespective of the overall stage of fan development.

In addition, our analyses have so far focused only on the effects of varying debris-flow magnitudes on avulsion and fan evolution, while in reality the debris-flow composition (and thus bulk or macro-scale rheology) may also vary between flows [e.g., *Suwa et al.*, 2009; *Okano et al.*, 2012; *De Haas et al.*, 2015b]. For example, flows with a composition that renders them more immobile, such as low water content or high cobble to boulder fraction [e.g., *De Haas et al.*, 2015b], may be more likely to cause channel plugging and induce avulsion. Such behavior has been documented on the Kamikamihori fan, where debris flows with a bouldery, matrix-poor, flow front were observed to be relatively immobile and therefore prone to deposit near the fan apex, jamming the channel and triggering avulsion in subsequent flows [*Okuda et al.*, 1981; *Suwa and Yamakoshi*, 1999; *Suwa et al.*, 2009]. The impact of debris-flow composition on avulsion mechanisms remains an important avenue towards a better understanding of fan evolution.

4.2 Compensational tendency and implication for flow routing

The compensation index increased from ∼0.25 at the fan apex to ∼0.35 near the fan toe on the three experimental debris-flow fans over temporal intervals of 1 to 20 flows (Fig. 10).

This suggests that debris-flow deposition at the scale of one to a few flows fell between anti-compensational and random tendencies, and that over such short time scales flows were likely to follow the existing topographic pathway. Depositional behavior became somewhat more compensational with increasing distance from the fan apex. Beyond a time scale of about 10-20 events, however, avulsion (whether initiated by a channel plug or a backstepping sequence, as described above) often tended to redirect flow towards a topographically low area on the fan. *Straub et al.* [2009] showed that fan systems dominated by gradual lateral shifting of the depocentre, punctuated by infrequent large-scale avulsion to the absolute topographic low, tend towards a compensation index of $\sim$0.3, similar to the values estimated here.

De Haas et al. [2018] observed that compensational behavior on natural debris-flow fans typically occurs only across sequences of flows, rather than between successive flows, again in agreement with our experimental observations. Debris flows on the Kamikamihori fan in Japan, for example, have been observed to occupy a channel for periods of a few flows until deposition shifts towards a topographically lower part on the fan [e.g., *Okuda et al.*, 1981; *Suwa and Okuda*, 1983; *Suwa and Yamakoshi*, 1999; *De Haas et al.*, 2018]. Similarly, such flow routing patterns are expressed in the surface topography of many modern debris-flow fans. We illustrate this behavior with a debris-flow fan from Saline Valley in the southwestern USA. The two most recent channel pathways on this fan have formed by persistent deposition over multiple flows, as inferred from the surface morphology (Fig. 11a, b). This persistent depositional activity has led to channel superelevation of $\sim$2-8 m (see topographic profiles A-A' to D-D' in Figure 11), which substantially exceeds the $\sim$1-3 m channel depth. For comparison, *Mohrig et al.* [2000] found that fluvial channel levees rarely aggrade more than 0.6 times the channel depth before avulsion. Thus, we tentatively hypothesize that debris-flow fans may be characterized by more persistent, anti-compensational depositional behavior compared to their fluvial counterparts. On the other hand, the stochastic nature and formation of channel plugs can allow for rapid and unexpected channel shifting on debris-flow fans, without the need for widespread backfilling of accommodation, and enhancing the degree of compensation. On three debris-flow fans in Colorado, USA, *Pederson et al.* [2015] found intermediate to fully compensational stacking patterns (compensation indices $\sim$0.6-1). The compensational tendency of these fans appeared to increase with flow thickness, flow width, abundance of coarse clasts, percentage of clay and distance from the fan apex, all of which were inferred to increase the likelihood of avulsion out of the active channel. Our experiments are at least partly consistent with these observations, as avulsions were promoted by wider, thicker flows, and the experimental compensation index increased toward the fan toes. The dependencies of avulsion behavior on both flow magnitude and composition make it difficult to attribute one mode of compensational behavior to all debris-flow fans, and highlight the need for more systematic understanding of the link between flow characteristics and compensation.

4.3 Implications for debris-flow hazard mitigation

Debris-flow avulsions are generally difficult to predict, and may therefore have substantial hazardous effects. The experimental results, however, provide some guidelines for identifying and mitigating potential avulsions. Small to moderately-sized debris flows are unlikely to leave the main channel and cause avulsion, but they can be important avulsion precursors or triggers. Avulsion is highly likely to occur when the snouts of one or a series of small to moderately-sized flows have jammed the proximal channel. Avulsion can then be expected to occur just upstream of the channel plug in the next large debris flow. In addition, large flows have been observed to create levee breaches and potential new channel locations during overbank surges, thus creating the template for an imminent avulsion in a large subsequent flow. In terms of hazard mitigation, it is thus important to check for potential channel plugs after small to moderate-sized flows, and for levee breaches and the onset of potential new channels after large events. The tendency of avulsions to re-occupy older channels on the flow surface, and thus for channels to act as flow attractors, should also be considered when assessing potential debris-flow hazard.

Our experimental observation that plugging and backstepping are favored during small- to medium-sized flows, while avulsion subsequently occurs during the next large flow, supports the hypothesis of *De Haas et al.* [2018] that there may be an optimal magnitude-frequency distribution for which avulsion frequency is maximized. For hazard mitigation it is important to understand which types of magnitude-frequency distribution result in a high avulsion frequency. Although still far from a definitive answer, our experimental results suggest that such a favorable distribution likely includes sufficient small- to moderately-sized debris flows to cause channel plugs and induce backstepping sequences, but also sufficient large flows to enable the formation of new pathways. Systems in which large flows are relatively abundant may be less prone to avulsion because of the paucity of smaller, plug-forming flows and the tendency of large flows to entrain material and thus enlarge the main channel as they transit the fan [*Schürch et al.*, 2011]. On the other hand, a proportional deficiency of large flows may also result in a lower avulsion frequency, because there are fewer flows with sufficient size to leave the main channel and form a new channel. At present, we lack the data on flow magnitude-frequency distributions from natural debris-flow fans with which to test these ideas, but such distributions would be an important research target in the near future.

5 Conclusions

This paper investigates how patterns of debris-flow fan avulsion and evolution are affected by the magnitude-frequency distribution of the flows. We compared the topographic evolution, avulsion mechanisms, and compensational tendencies, of three experimental fans formed by contrasting flow magnitude-frequency distributions: (1) a uniform distribution, (2) a steep double-Pareto distribution with many flows around the mean and a limited number of large flows, and (3) a shallow double-Pareto distribution with fewer flows around the mean and more abundant large flows.

The three experimental fans followed similar overall patterns of development, evolving through alternating channelized and unchannelized phases that were governed by sequences of backstepping deposition and avulsion. In detail, however, the differences in magnitude-frequency distribution also caused marked differences in the avulsion mechanisms, and thus surface evolution, of the three fans. The fan formed by uniform flows developed through regular sequences of channelization, backstepping from fan toe to fan apex, and avulsion over multiple flows. In contrast, large debris flows on the fans formed by a double-Pareto distribution were observed to overtop the active channel and carve new flow paths through the channel levees, at times initiating avulsion within a single event. On these fans, avulsions were also triggered by series of similarly-sized or progressively smaller flows which plugged the active channel, leading to avulsion in the next large flow. This latter mechanism was far more common on the fan formed by a steep double-Pareto distribution, which we attribute to both (1) the predominance of moderate flows on this fan and (2) the relative abundance of large flows on the fan formed by the shallow double-Pareto distribution that kept the channel clear. On all experimental fans, backstepping sequences were either initiated after filling of regional accommodation or plug formation, and the relative importance of these processes largely depended on the debris-flow magnitude-frequency distribution.

In short, channel plugs were more likely to be formed by small- to moderately-sized flows, whereas large flows were more prone to leave the main channel and initiate or exploit a new pathway down the fan. We infer that there is likely to be an optimal magnitude-frequency distribution that maximizes the avulsion frequency, reflecting a balance between small- to medium-sized flows that can plug the channel and induce backstepping, and large flows that subsequently avulse out of the main channel.

Our results provide some guidelines for avulsion hazard mitigation; sequences of small- to moderately-sized flows, especially those that deposit material within the active channel, may serve as precursors to avulsion on natural fans. Similarly, large flows that cause levee breaches and incipient development of new channel pathways should also be treated as avulsion precursors.

Acknowledgments

We thank the Associate Editor and two anonymous reviewers for constructive and insightful comments that improved the focus and clarity of the paper. TdH was funded by the Netherlands Organization for Scientific Research (NWO) via Rubicon grant 019.153LW.002. ALD acknowledges funding from the Institute of International Education via the Global Innovation Initiative program. We thank Kimberly Hill, Gordon Zhou, Qicheng Sun, and Brian McArdell for stimulating discussions on different aspects of this work.

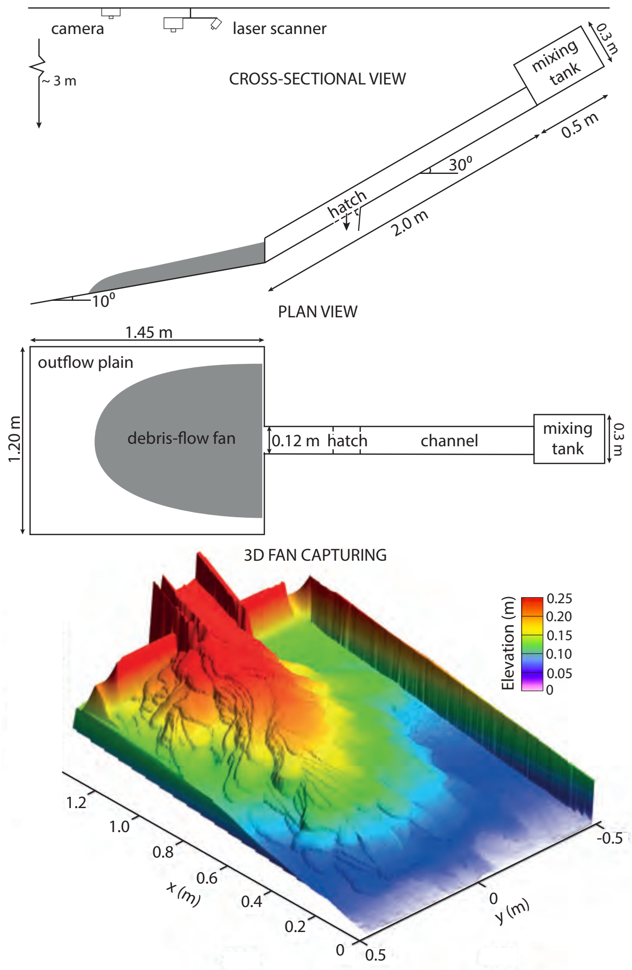

Figure 1: Experimental flume setup. The 3D fan image shows the final morphology of fan 01. The flume setup is similar to that used in *De Haas et al.* [2015b] and *De Haas et al.* [2016]. Figure modified from *De Haas et al.* [2016].

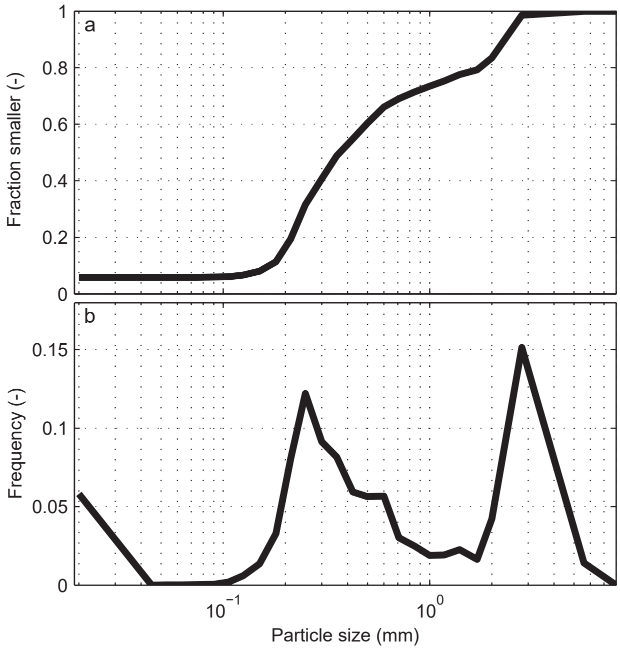

Figure 2: Particle-size distribution of the debris flows forming the experimental fans. (a) Cumulative distribution. (b) Frequency distribution.

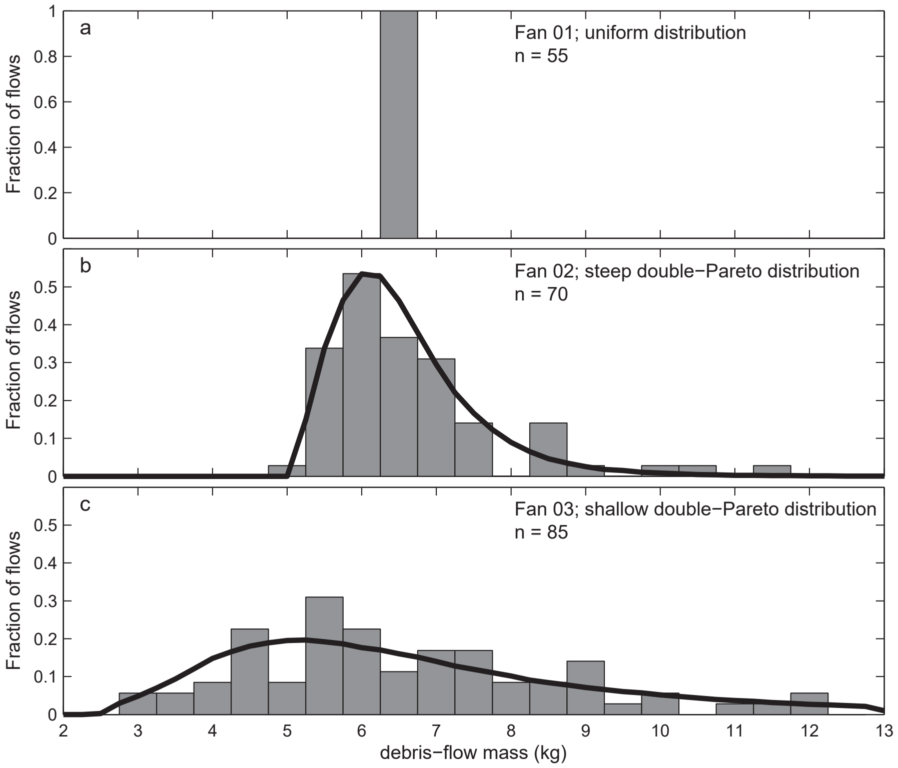

Figure 3: Magnitude-frequency distributions of the experimental debris-flow fans. The lines denote the double-Pareto distributions from which the debris-flow magnitudes were randomly extracted. The bars denote the actual number of events in each experiment, divided into 0.5 kg bins. The mean debris-flow mass is $\sim$6.5 kg for all experiments. (a) Fan 01 with a uniform distribution; (b) fan 02 with a steep-tailed double-Pareto distribution; (c) fan 03 with a shallow-tailed double-Pareto distribution.

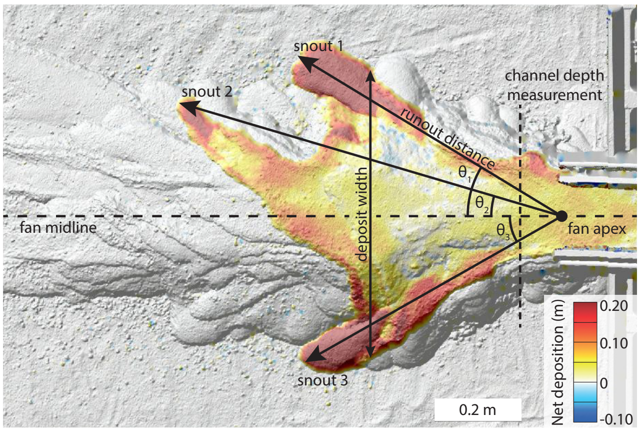

Figure 4: Depositional geometry and measurement of spatio-temporal patterns of debris-flow activity. For each snout, the runout distance is the distance between snout front and fan apex, and the flow angle is the angle between the fan midline and a straight line between debris-flow snout and apex. Deposit width is defined as the maximum width of the deposit, excluding individual snouts substantially outside of the main flow direction. Channel depth is measured 10 cm downstream of the fan apex.

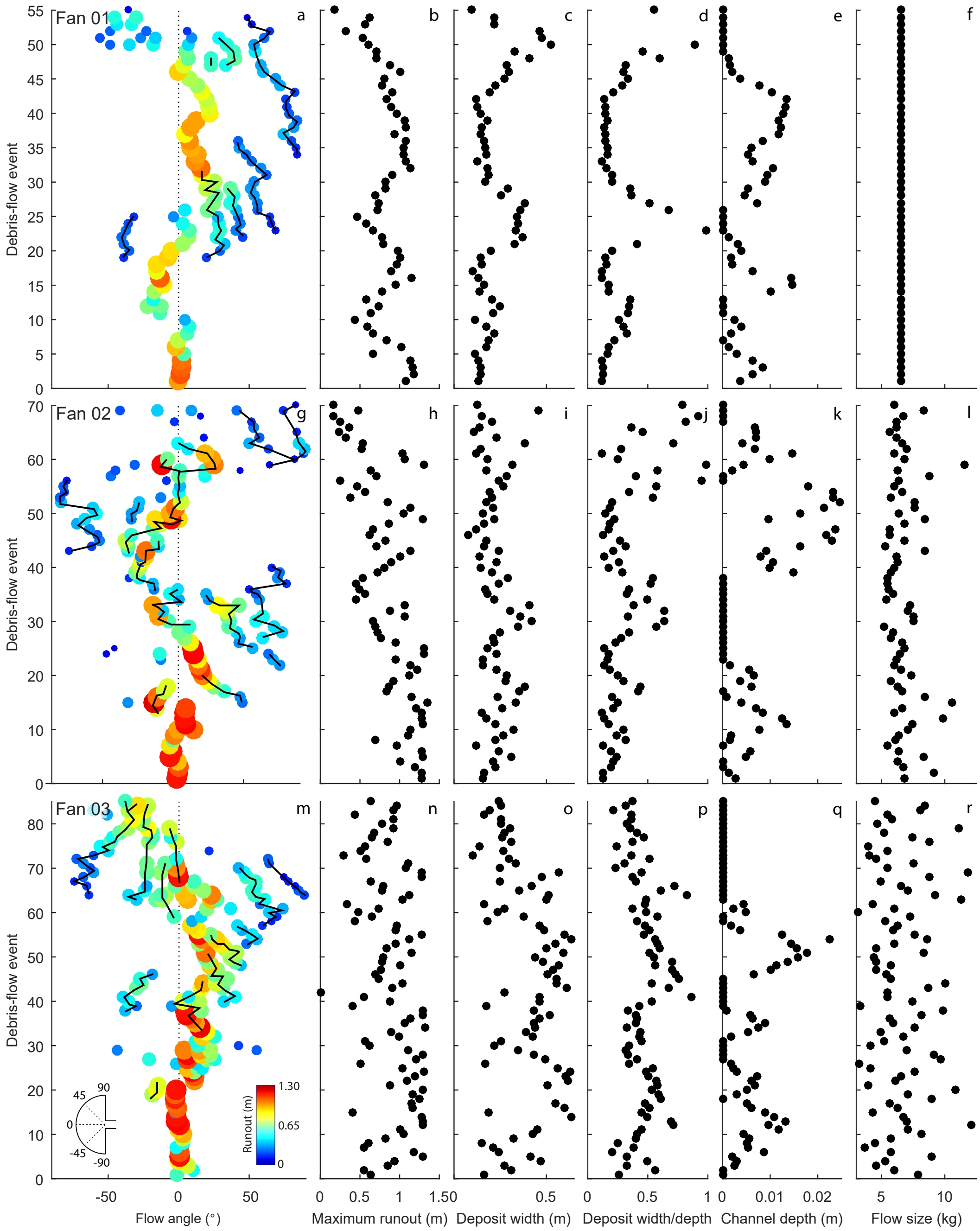

Figure 5: Summary of the spatio-temporal patterns of debris-flow activity on fans 01-03. (a) Flow angle and runout distance of the channels active during the debris-flow events that formed fan 01. Flow angle was previously published in *De Haas et al.* [2016]; the other variables are newly reported here. Solid line segments join successive flows in the same channel. (b) Maximum runout distance during each debris flow on fan 01. (c) Deposit width during each event on fan 01. (d) Deposit width/depth ratio for each debris flow on fan 01, defined as deposit width divided by maximum runout distance. (e) Channel depth after each debris-flow event on fan 01, measured 10 cm downstream of the fan apex. (f) Debris-flow mass in kg. (g-l) As above for fan 02. (m-r) As above for fan 03.

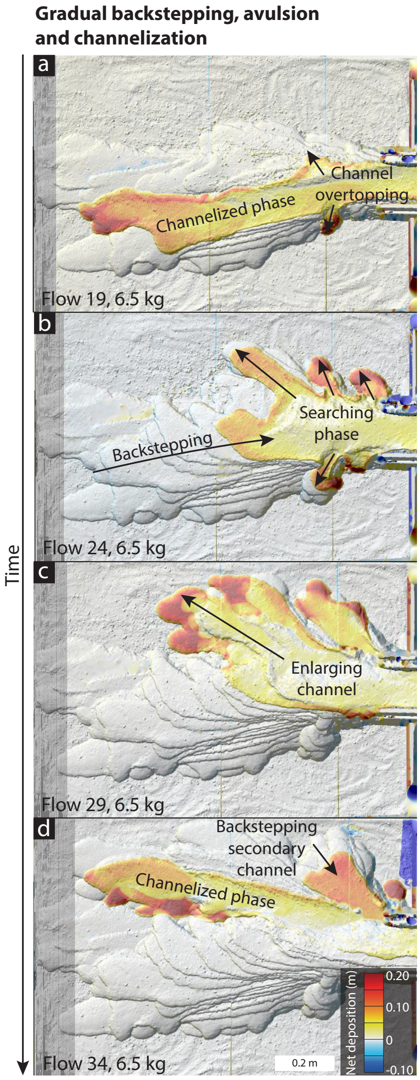

Figure 6: Typical avulsion sequence on fan 01, formed by a uniform flow magnitude-frequency distribution (Fig. 3a). The sequence shows evolution from a well-defined channel (panel a) through gradual backstepping of deposition toward the fan apex, followed by a searching phase (panel b), avulsion to a new channel pathway and enlargement (panel c), and channelization (panel d). Note that a secondary channel formed but was plugged and abandoned during this sequence.

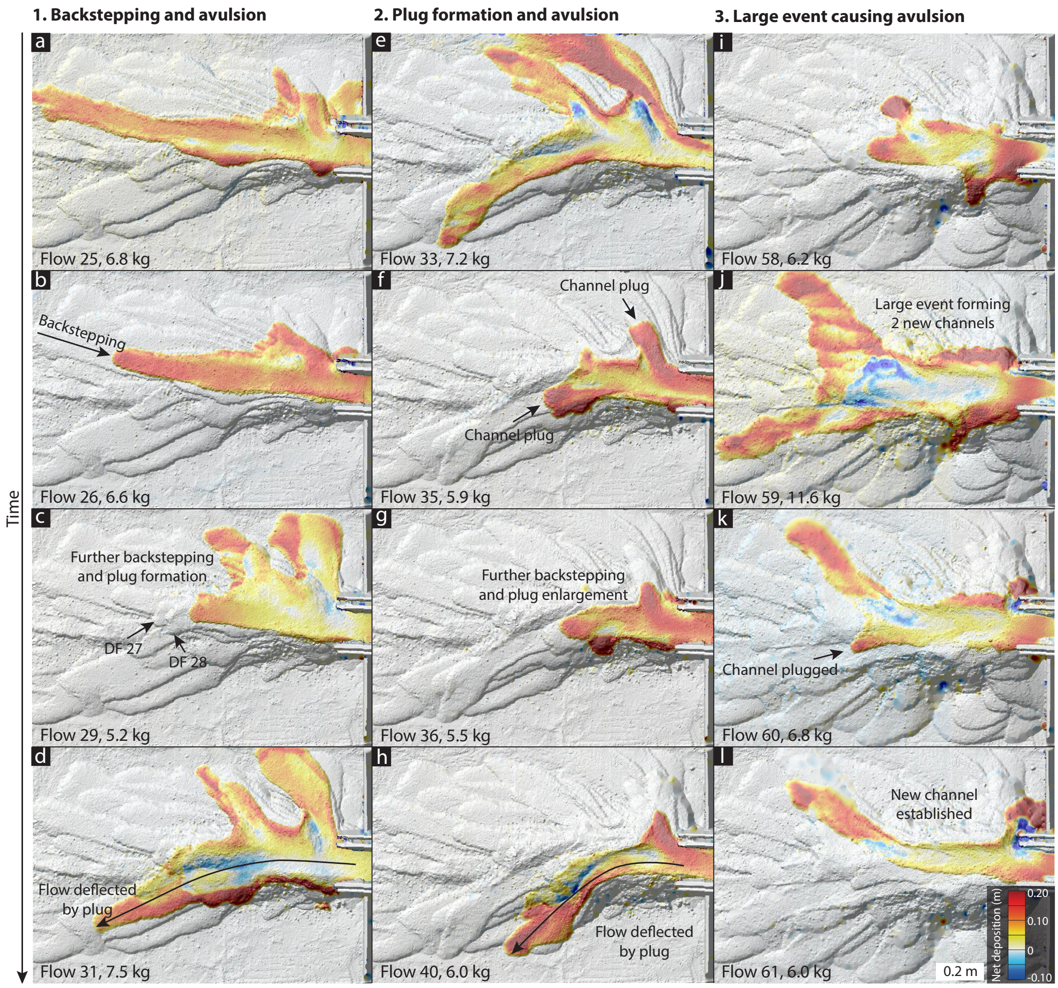

Figure 7: Common debris-flow-magnitude sequences leading to avulsion on fan 02, formed by a steep-tailed double-Pareto flow distribution (Fig. 3b). (a-d) Backstepping and avulsion sequence during debris flows 25-31. A sequence of small- to moderately-sized flows induced a sequence of backstepping deposition (panels b to c), which was followed by avulsion during the large flow 31 (panel d). (e-h) Channel plug formation by two small debris flows that blocked the main channel (panels f and g), followed by avulsion during a moderately-sized flow (panel h). (i-l) A very large debris flow created two new channels (panel j), one of which became blocked by a flow snout in the next, smaller flow (panel k). Avulsion then proceeded into the topographically-favored right-hand channel (panel l).

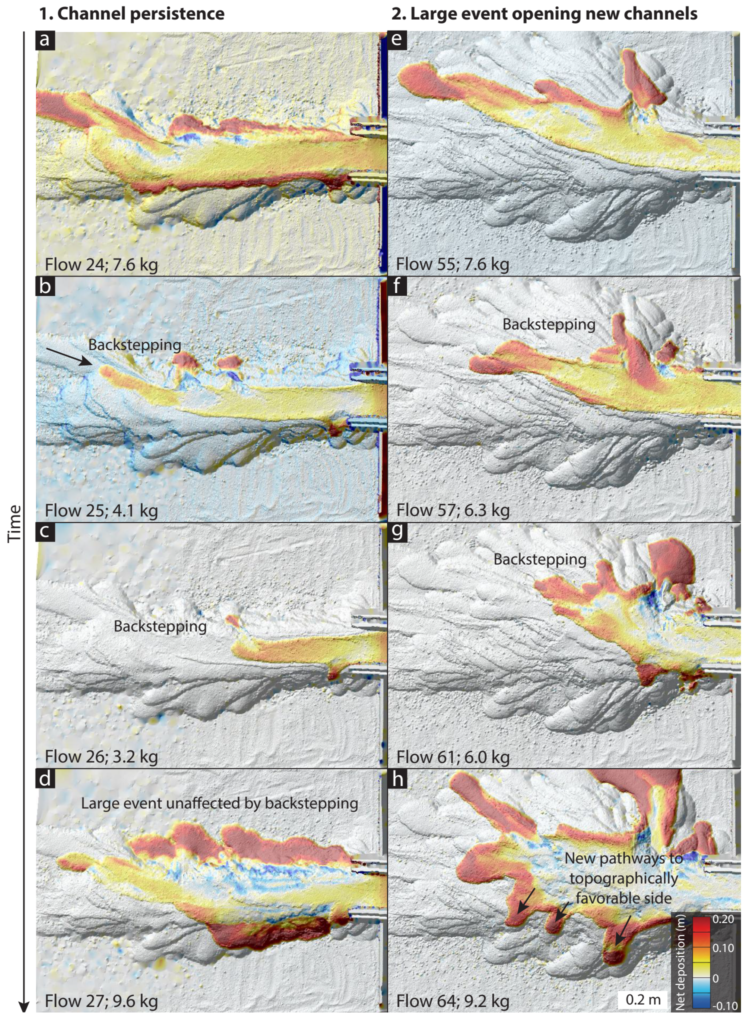

Figure 8: Common spatio-temporal patterns of debris-flow activity on fan 03, formed by a shallow-tailed double-Pareto flow distribution (Fig. 3c). (a-d) Persistent channel position during debris flows 24-27. The direction of the large debris flow 27 (panel d) was unaffected by the backstepping plug deposits from the small flows 25 and 26 (panels b and c). Flow 27 partly eroded the channel plug and filled the channel surrounding the plug. Overbank surges were widespread during the relatively large flows 24 and 27 (panels a and d). (e-h) After a partial backstepping sequence from debris flow 55 to 62 (panels e-g), large flows 63 and 64 opened up three new channel pathways on the left side of the fan (panel h, shown by arrows) that allowed subsequent avulsion towards the left.

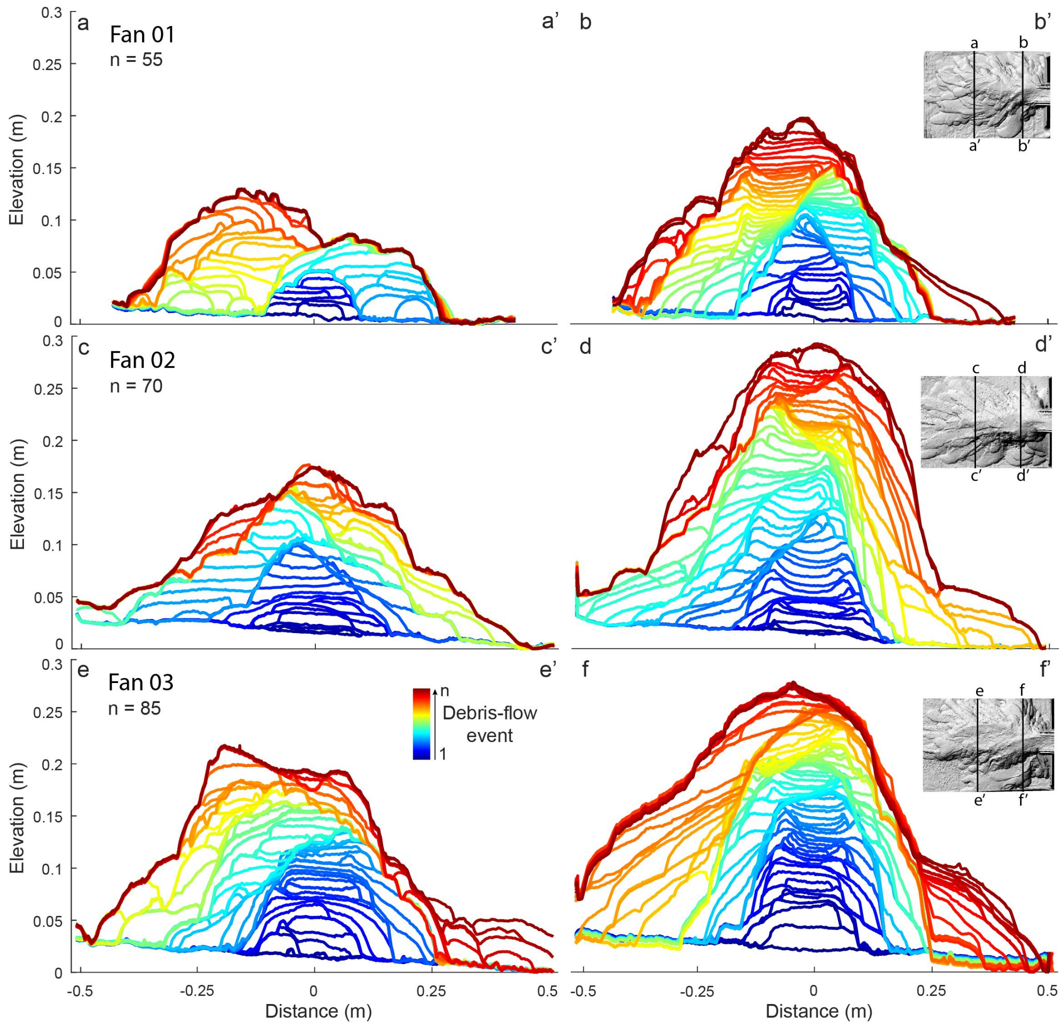

Figure 9: Cross-profiles through the experimental debris-flow fans at distances of 0.2 m (left-hand column) and 0.8 m (right-hand column) downstream of the fan apex. Colors show progressive flow sequence from cool to warm. (a-b) Fan 01, previously shown in *De Haas et al.* [2016]. (c-d) Fan 02. (e-f) Fan 03. Note how overbank deposition became increasingly important for fan construction and how large lateral shifts became less pronounced with increasing flow-magnitude variability from fan 01 to 03.

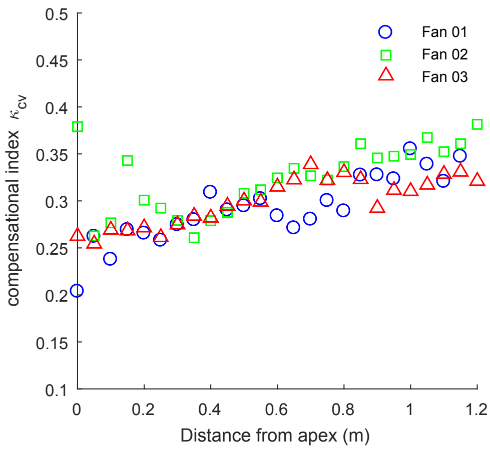

Figure 10: Compensation index from fan apex (left) to fan toe (right) for fans 01-03.

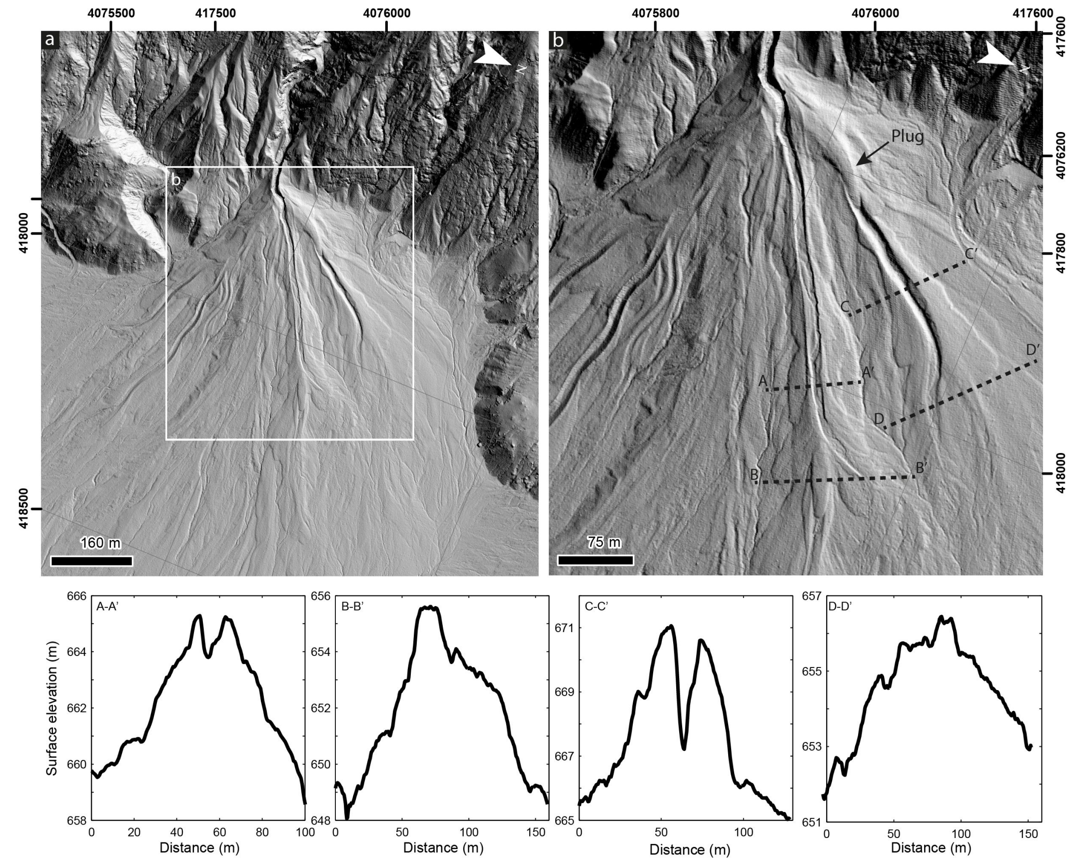

Figure 11: Channel superelevation on a debris-flow fan in southern Saline Valley, California, USA. Panels (a) and (b) show present-day topography of the fan surface. Data are from the EarthScope Southern & Eastern California Lidar Project ($www.opentopography.org$) with a cell size of 0.5 m. The cross-sections below show the absolute superelevation of the two most recently-active channels on the fan. This example shows how deposits can act as attractors, mainly due to the presence of an incised apex channel, leading to superelevation of 2-8 m. Coordinates in UTM WGS 1984 11N.

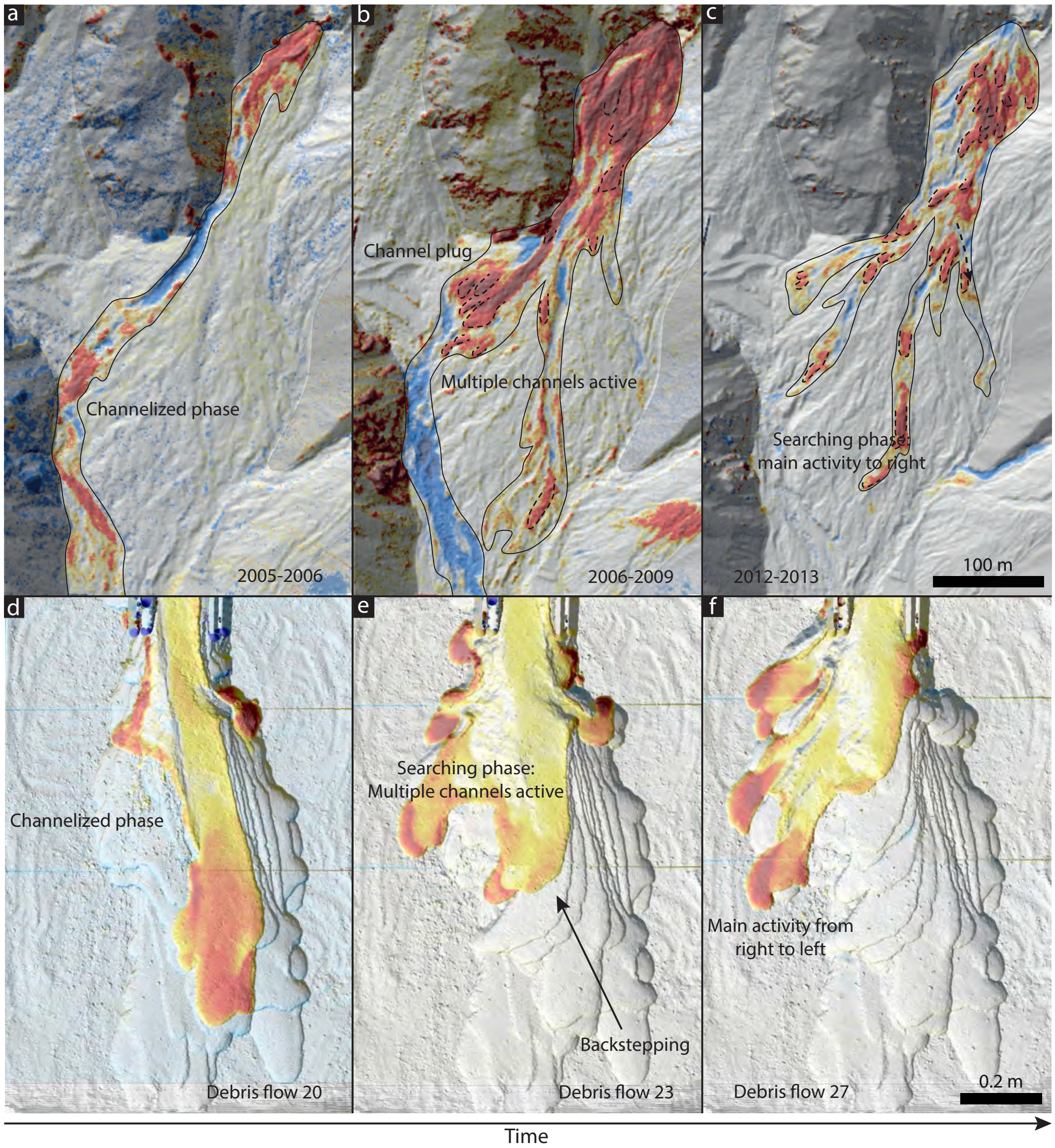

Figure 12: Examples of the transition from channelized to searching phases on (a-c) the Ohya debris-flow fan in Japan [images modified from *Imaizumi et al.*, 2016; *De Haas et al.*, 2018] and (d-f) experimental debris-flow fan 01. Flow in all panels was from top to bottom. On both the natural and experimental fans, activity during the searching phase was spread over multiple channels on the proximal fan, and the locus of activity shifted laterally across the fan over multiple debris flows. Warm colors indicate deposition and cool colors indicate erosion, although absolute scales differ.

References

Aslan, A., W. J. Autin, and M. D. Blum (2005), Causes of river avulsion: insights from the late Holocene avulsion history of the Mississippi River, USA, *Journal of Sedimentary Research*, *75*(4), 650–664.

Bardou, E., and M. Jaboyedoff (2008), Debris flows as a factor of hillslope evolution controlled by a continuous or a pulse process?, *Geological Society, London, Special Publications*, *296*(1), 63–78.

Beaty, C. B. (1963), Origin of alluvial fans, White Mountains, California and Nevada, *Ann. Assoc. Am. Geogr.*, *53*(4), 516–535.

Bennett, G., P. Molnar, H. Eisenbeiss, and B. McArdell (2012), Erosional power in the Swiss Alps: characterization of slope failure in the Illgraben, *Earth Surface Processes and Landforms*, *37*(15), 1627–1640.

Bennett, G., P. Molnar, B. McArdell, F. Schlunegger, and P. Burlando (2013), Patterns and controls of sediment production, transfer and yield in the Illgraben, *Geomorphology*, *188*, 68–82.

Bennett, G., P. Molnar, B. McArdell, and P. Burlando (2014), A probabilistic sediment cascade model of sediment transfer in the Illgraben, *Water Resources Research*, *50*(2), 1225–1244.

Blair, T. C., and J. G. McPherson (1994), Alluvial fans and their natural distinction from rivers based on morphology, hydraulic processes, sedimentary processes, and facies assemblages, *Journal of Sedimentary Research*, *64A*, 450–489.

Blair, T. C., and J. G. McPherson (2009), Processes and forms of alluvial fans, in *Geomorphology of Desert Environments*, edited by A. Parsons and A. Abrahams, pp. 413–467, Springer Netherlands.

Bollschweiler, M., M. Stoffel, and D. M. Schneuwly (2008), Dynamics in debris-flow activity on a forested cone - a case study using different dendroecological approaches, *Catena*, *72*(1), 67–78.

Brizga, S. O., and B. L. Finlayson (1990), Channel avulsion and river metamorphosis: the case of the Thomson River, Victoria, Australia, *Earth Surface Processes and Landforms*, *15*(5), 391–404.

Cannon, S. H., J. E. Gartner, R. C. Wilson, J. C. Bowers, and J. L. Laber (2008), Storm rainfall conditions for floods and debris flows from recently burned areas in southwestern Colorado and southern California, *Geomorphology*, *96*(3), 250–269.

Cannon, S. H., E. M. Boldt, J. L. Laber, J. W. Kean, and D. M. Staley (2011), Rainfall intensity–duration thresholds for postfire debris-flow emergency-response planning, *Natural Hazards*, *59*(1), 209–236.

Clague, J. J., C. Huggel, O. Korup, and B. McGuire (2012), Climate change and hazardous processes in high mountain, *Revista de la Asociación Geológica Argentina*, *69*(3), 328–338.

Clarke, L., T. A. Quine, and A. Nicholas (2010), An experimental investigation of autogenic behaviour during alluvial fan evolution, *Geomorphology*, *115*(3), 278–285.

Dai, F., and C. Lee (2001), Frequency–volume relation and prediction of rainfall-induced landslides, *Engineering geology*, *59*(3), 253–266.

D'Arcy, M., D. C. Roda Boluda, A. C. Whittaker, and A. Carpineti (2015), Dating alluvial fan surfaces in Owens Valley, California, using weathering fractures in boulders, *Earth Surface Processes and Landforms*, *40*(4), 487–501.

De Haas, T., and T. Van Woerkom (2016), Bed scour by debris flows: experimental investigation of effects of debris-flow composition, *Earth Surface Processes and Landforms*, *41*(13), 1951–1966, doi:10.1002/esp.3963, esp.3963.

De Haas, T., D. Ventra, P. E. Carbonneau, and M. G. Kleinhans (2014), Debris-flow dominance of alluvial fans masked by runoff reworking and weathering, *Geomorphology*, *217*, 165–181.

De Haas, T., M. G. Kleinhans, P. E. Carbonneau, L. Rubensdotter, and E. Hauber (2015a), Surface morphology of fans in the high-Arctic periglacial environment of Svalbard: Controls and processes, *Earth-Science Reviews*, *146*, 163–182.

De Haas, T., L. Braat, J. F. W. Leuven, I. R. Lokhorst, and M. G. Kleinhans (2015b), Effects of debris-flow composition and topography on runout distance, depositional mechanisms and deposit morphology, *Journal of Geophysical Research: Earth Surface*, *120*, 1949–1972.

De Haas, T., W. Berg, L. Braat, and M. G. Kleinhans (2016), Autogenic avulsion, channelization and backfilling dynamics of debris-flow fans, *Sedimentology*, *63*, 1596–1619.

De Haas, T., A. L. Densmore, M. Stoffel, H. Suwa, F. Imaizumi, J. A. Ballesteros-Cánovas, and T. Wasklewicz (2018), Avulsions and the spatio-temporal evolution of debris-flow fans, *Earth Science Reviews*, *177*, 53–75, doi:10.1016/j.earscirev.2017.11.007.

Dühnforth, M., A. L. Densmore, S. Ivy-Ochs, P. A. Allen, and P. W. Kubik (2007), Timing and patterns of debris flow deposition on Shepherd and Symmes creek fans, Owens Valley, California, deduced from cosmogenic 10Be, *Journal of Geophysical Research: Earth Surface (2003–2012)*, *112*(F3).

Dühnforth, M., A. L. Densmore, S. Ivy-Ochs, and P. A. Allen (2008), Controls on sediment evacuation from glacially modified and unmodified catchments in the eastern Sierra Nevada, California, *Earth Surface Processes and Landforms*, *33*(10), 1602–1613.

Edmonds, D. A., D. C. Hoyal, B. A. Sheets, and R. L. Slingerland (2009), Predicting delta avulsions: Implications for coastal wetland restoration, *Geology*, *37*(8), 759–762.

Ganti, V., Z. Chu, M. P. Lamb, J. A. Nittrouer, and G. Parker (2014), Testing morphodynamic controls on the location and frequency of river avulsions on fans versus deltas: Huanghe (Yellow River), China, *Geophysical Research Letters*, *41*(22), 7882–7890.

Ganti, V., A. J. Chadwick, H. J. Hassenruck-Gudipati, and M. P. Lamb (2016), Avulsion cycles and their stratigraphic signature on an experimental backwater-controlled delta, *Journal of Geophysical Research: Earth Surface*, *121*(9), 1651–1675.

Guthrie, R., and S. Evans (2004), Analysis of landslide frequencies and characteristics in a natural system, coastal British Columbia, *Earth Surface Processes and Landforms*, *29*(11), 1321–1339.

Hamilton, P. B., K. Strom, and D. C. Hoyal (2013), Autogenic incision-backfilling cycles and lobe formation during the growth of alluvial fans with supercritical distributaries, *Sedimentology*, *60*(6), 1498–1525.

Harvey, A. (2011), Dryland alluvial fans, *Arid Zone Geomorphology: Process, Form and Change in Drylands, Third Edition*, pp. 333–371.

Helsen, M. M., P. J. M. Koop, and H. Van Steijn (2002), Magnitude-frequency relationship for debris flows on the fan of the Chalance torrent, Valgaudemar (French Alps), *Earth Surface Processes and Landforms*, *27*(12), 1299–1307.

Hoefling, R. (2004), High-speed 3D imaging by DMD technology, in *Electronic Imaging 2004*, pp. 188–194, International Society for Optics and Photonics.

Hooke, R. B., and W. L. Rohrer (1979), Geometry of alluvial fans: Effect of discharge and sediment size, *Earth Surface Processes*, *4*(2), 147–166.

Hooke, R. L. (1967), Processes on arid-region alluvial fans, *The Journal of Geology*, pp. 438–460.

Hovius, N., C. P. Stark, and P. A. Allen (1997), Sediment flux from a mountain belt derived by landslide mapping, *Geology*, *25*(3), 231–234.

Huang, R., and X. Fan (2013), The landslide story, *Nature Geoscience*, *6*(5), 325–326.

Hungr, O., S. Evans, and J. Hazzard (1999), Magnitude and frequency of rock falls and rock slides along the main transportation corridors of southwestern British Columbia, *Canadian Geotechnical Journal*, *36*(2), 224–238.

Imaizumi, F., D. Trappmann, N. Matsuoka, S. Tsuchiya, O. Ohsaka, and M. Stoffel (2016), Biographical sketch of a giant: Deciphering recent debris-flow dynamics from the Ohya landslide body (Japanese Alps), *Geomorphology*, *272*, 102–114.

Iverson, R. M. (1997), The physics of debris flows, *Reviews of Geophysics*, *35*(3), 245–296.

Iverson, R. M., M. E. Reid, M. Logan, R. G. LaHusen, J. W. Godt, and J. P. Griswold (2011), Positive feedback and momentum growth during debris-flow entrainment of wet bed sediment, *Nature Geoscience*, *4*(2), 116–121.

Ma, C., Y. Wang, K. Hu, C. Du, and W. Yang (2017), Rainfall intensity–duration threshold and erosion competence of debris flows in four areas affected by the 2008 Wenchuan earthquake, *Geomorphology*, *282*, 85–95.

Malamud, B. D., D. L. Turcotte, F. Guzzetti, and P. Reichenbach (2004), Landslide inventories and their statistical properties, *Earth Surface Processes and Landforms*, *29*(6), 687–711.

Mohrig, D., P. L. Heller, C. Paola, and W. J. Lyons (2000), Interpreting avulsion process from ancient alluvial sequences: Guadalope-matarranya system (northern spain) and wasatch formation (western colorado), *Geological Society of America Bulletin*, *112*(12), 1787–1803.

Okano, K., H. Suwa, and T. Kanno (2012), Characterization of debris flows by rainstorm condition at a torrent on the Mount Yakedake volcano, Japan, *Geomorphology*, *136*(1), 88–94.

Okuda, S., S. Suwa, K. Okunishi, and K. Yokoyama (1981), Depositional processes of debris flow at Kamikamihori fan, Northern Japan Alps, *Trans. Japan. Geomorph. Union*, *2*, 353–361.

Paola, C., K. Straub, D. Mohrig, and L. Reinhardt (2009), The unreasonable effectiveness of stratigraphic and geomorphic experiments, *Earth-Science Reviews*, *97*(1), 1–43.

Pederson, C. A., P. M. Santi, and D. R. Pyles (2015), Relating the compensational stacking of debris-flow fans to characteristics of their underlying stratigraphy: Implications for geologic hazard assessment and mitigation, *Geomorphology*, *248*, 47–56.

Powell, E. J., W. Kim, and T. Muto (2012), Varying discharge controls on timescales of autogenic storage and release processes in fluvio-deltaic environments: Tank experiments, *Journal of Geophysical Research: Earth Surface*, *117*(F02011).

Rebetez, M., R. Lugon, and P.-A. Baeriswyl (1997), Climatic change and debris flows in high mountain regions: the case study of the Ritigraben torrent (Swiss Alps), *Climatic change*, *36*(3-4), 371–389.

Reed, W. J. (2001), The pareto, zipf and other power laws, *Economics Letters*, *74*(1), 15–19.

Reed, W. J., and M. Jorgensen (2004), The double pareto-lognormal distributiona new parametric model for size distributions, *Communications in Statistics-Theory and Methods*, *33*(8), 1733–1753.

Reitz, M. D., D. J. Jerolmack, and J. B. Swenson (2010), Flooding and flow path selection on alluvial fans and deltas, *Geophysical Research Letters*, *37*(6), L06,401.

Schumm, S., M. Mosley, and W. Weaver (1987), *Experimental Fluvial Geomorphology*, John Wiley and Sons, New York.

Schürch, P. (2011), Debris-flow erosion and deposition dynamics, Ph.D. thesis, Durham University.

Schürch, P., A. L. Densmore, N. J. Rosser, and B. W. McArdell (2011), Dynamic controls on erosion and deposition on debris-flow fans, *Geology*, *39*(9), 827–830.

Schürch, P., A. L. Densmore, S. Ivy-Ochs, N. J. Rosser, F. Kober, F. Schlunegger, B. McArdell, and V. Alfimov (2016), Quantitative reconstruction of late Holocene surface evolution on an alpine debris-flow fan, *Geomorphology*, *275*, 46–57.

Shieh, C.-L., Y. Chen, Y. Tsai, and J. Wu (2009), Variability in rainfall threshold for debris flow after the Chi-Chi earthquake in central Taiwan, China, *International Journal of Sediment Research*, *24*(2), 177–188.

Slingerland, R., and N. D. Smith (1998), Necessary conditions for a meandering-river avulsion, *Geology*, *26*(5), 435–438.

Stark, C. P., and N. Hovius (2001), The characterization of landslide size distributions, *Geophysical Research Letters*, *28*(6), 1091–1094.

Stoffel, M. (2010), Magnitude–frequency relationships of debris flows-a case study based on field surveys and tree-ring records, *Geomorphology*, *116*(1), 67–76.

Stoffel, M., D. Conus, M. A. Grichting, I. Lièvre, and G. Maître (2008), Unraveling the patterns of late Holocene debris-flow activity on a cone in the Swiss Alps: chronology, environment and implications for the future, *Global and Planetary Change*, *60*(3), 222–234.

Straub, K. M., and D. R. Pyles (2012), Quantifying the hierarchical organization of compensation in submarine fans using surface statistics, *Journal of Sedimentary Research*, *82*(11), 889–898.

Straub, K. M., C. Paola, D. Mohrig, M. A. Wolinsky, and T. George (2009), Compensational stacking of channelized sedimentary deposits, *Journal of Sedimentary Research*, *79*(9), 673–688.

Suwa, H., and S. Okuda (1983), Deposition of debris flows on a fan surface, Mt. Yakedake, Japan, *Zeitschrift fur Geomorphologie NF Supplementband*, *46*, 79–101.

Suwa, H., and T. Yamakoshi (1999), Sediment discharge by storm runoff at volcanic torrents affected by eruption, *Zeitschrift fur Geomorphologie NF Supplementband*, *114*, 63–88.

Suwa, H., K. Okano, and T. Kanno (2009), Behavior of debris flows monitored on test slopes of Kamikamihorizawa Creek, Mount Yakedake, Japan, *International Journal of Erosion Control Engineering*, *2*(2), 33–45.

Van Dijk, M., G. Postma, and M. G. Kleinhans (2009), Autocyclic behaviour of fan deltas: an analogue experimental study, *Sedimentology*, *56*(5), 1569–1589.

Van Dijk, M., M. G. Kleinhans, G. Postma, and E. Kraal (2012), Contrasting morphodynamics in alluvial fans and fan deltas: effect of the downstream boundary, *Sedimentology*, *59*(7), 2125–2145.

Wang, Y., K. M. Straub, and E. A. Hajek (2011), Scale-dependent compensational stacking: an estimate of autogenic time scales in channelized sedimentary deposits, *Geology*, *39*(9), 811–814.

Wasklewicz, T., and C. Scheinert (2016), Development and maintenance of a telescoping debris flow fan in response to human-induced fan surface channelization, Chalk Creek Valley Natural Debris Flow Laboratory, Colorado, USA, *Geomorphology*, *252*, 51–65.

Whipple, K. X., and T. Dunne (1992), The influence of debris-flow rheology on fan morphology, Owens Valley, California, *Geological Society of America Bulletin*, *104*(7), 887–900.

Zaginaev, V., J. Ballesteros-Cánovas, S. Erokhin, E. Matov, D. Petrakov, and M. Stoffel (2016), Reconstruction of glacial lake outburst floods in northern Tien Shan: Implications for hazard assessment, *Geomorphology*, *269*, 75–84.